

# Petrogenesis and tectonic affinities of Imorona-Itsindro gabbros in the Alaotra region of central Madagascar: whole rock analyses and geodynamic implications

Heninjara Narimihamina Rarivoarison<sup>1,2</sup>, Raymond Rakotondrazafy<sup>2</sup>, Nuria Sanchez-Pastor<sup>3</sup>

<sup>1</sup> Department of Applied Geosciences, German University of Technology in Oman, Sultanate of Oman

<sup>2</sup> Doctoral school of Earth Sciences and Evolution, Faculty of Sciences and Technology, University of Antananarivo, Madagascar

<sup>3</sup> Department of Mineralogy and Petrology, Faculty of Geological Sciences, University Complutense of Madrid, C/ José Antonio Novais, 12, Madrid 28040, Spain

## ABSTRACT

During the Cryogenian period (0.84–0.76 Ga), the bimodal Imorona-Itsindro plutonic suite intruded the Precambrian basement of Madagascar and has been the subject of continuous debate regarding its origin and tectonic setting. Controversy exists between studies proposing an intraplate rift related to the mantle plume and those favoring an Andean-type suprasubduction origin. This study focuses on the whole rock analyses of the Imorona-Itsindro gabbros in the Alaotra region to explain their magmatic and tectonic affinities, and their geodynamic implications. Sampling was carried out in three different sectors around Lake Alaotra. Eight gabbro samples were collected and subjected to major and trace element analyzes using ICP-OES and ICP-MS techniques. Petrographically, gabbros are mainly composed of plagioclase, olivine, clinopyroxene and orthopyroxene, with accessory minerals such as ilmenite, magnetite, spinel, pyrite, and apatite. The main oxide compositions show high Mg# tholeiitic affinity ( $46.93 < \text{Mg\#} < 74.24$ ), while variations between Mg# versus CaO indicate magmatic fractionation of plagioclase and clinopyroxene. Trace element compositions reveal light rare earth and large ion lithophile elements enrichments typical of subduction-related magmas, while high field strength elements show depletions, indicative of an underplate source. The results support an Andean-type suprasubduction setting consistent with a west-east vergence subduction between the Mozambique oceanic lithosphere and the Malagasy craton and its exotic terrains in this period.

**Keywords:** Cryogenian, bimodal plutonic suite, tholeiitic, underplate source, Andean-type subduction

## 1. INTRODUCTION

During the Cryogenian between 0.84 and 0.76 Ga, the Imorona-Itsindro bimodal plutonic suite intruded the Precambrian basement of Madagascar [1]. During that period, the oceanic lithosphere of the Mozambique ocean was gradually subducted beneath the western part of the Greater Dharwar craton as well as its exotic terrains [2]. Nature and origin of the melts have been disputed for a long time; therefore, two contrary arguments explain the origin of this magmatism: The first supports the presence of a mantle plume associated with an intraplate rift within the Dharwar region, as indicated by Tucker et al. [3], and Zhou et al. [4]; while the second is rather favorable to an Andean-type suprasubduction, as suggested by Collins and Windley [5] and Handke et al. [6]. This present study focuses on the whole rock geochemistry of the Imorona Itsindro gabbros located in the Alaotra-Mangoro region in order to better understand their magmatic and tectonic affinities, their geodynamic occurrences, and to provide new geochemical data.

## 2. GEOLOGICAL SETTING

Madagascar comprises a substantial Precambrian crystalline basement overlaid by Phanerozoic sedimentary layers (Roig et al., 2012). This basement is a composite of eight tectono-metamorphic domains (Fig - 1a.), each distinguished by its age, geological context, and rock properties [3]. The oldest domains, Antongil-Masora and Antananarivo, date back to the Archean era, around 3.5 billion years ago, forming the southeastern segment of the Greater Dharwar craton [3]. In the Paleoproterozoic, the Anosyan-Androyan domains joined the southern edge of the Greater Dharwar craton [3]. The Mesoproterozoic witnessed the formation of the Ikalamavony domain due to arc magmatism resulting from the gradual subduction of the pan-African oceanic lithosphere beneath the Dharwar craton, as well as the intrusion of the Dabolava magmatic suite [3]. Later, during the Cryogenian period, an intra-cratonic sedimentation phase formed the Ambatolampy and Manampotsy groups from detrital sediments sourced from Archean rocks, with additional magmatism creating the Imorona-Itsindro plutonic suite [1] as shown in Fig - 1b. In the Neoproterozoic, the Vohibory domain, an oceanic terrain associated with oceanic arc or fore-arc magmatism, accreted to the Androyan- Anosyan domains, while the Cryogenian Bemarivo domain merged with Antongil-Masora and Antananarivo domains in the northeast [3]. Following the amalgamation of Gondwana in the Upper Proterozoic, the Malagasy basement underwent substantial metamorphism and multiple deformations, accompanied by broad magmatic activity that gave rise to the Ambalavao-Kiangara-Maevarano magmatic suite [3]. Madagascar remained part of Gondwana during the Paleozoic but eventually separated from East Africa in the Upper Jurassic. Even during its isolation as an island in the Upper Cretaceous, around 90-65 million years ago, Madagascar experienced active lateral extension, resulting in the formation of sedimentary basins like the Alaotra Basin, exemplified by the creation of Lake Alaotra [7].

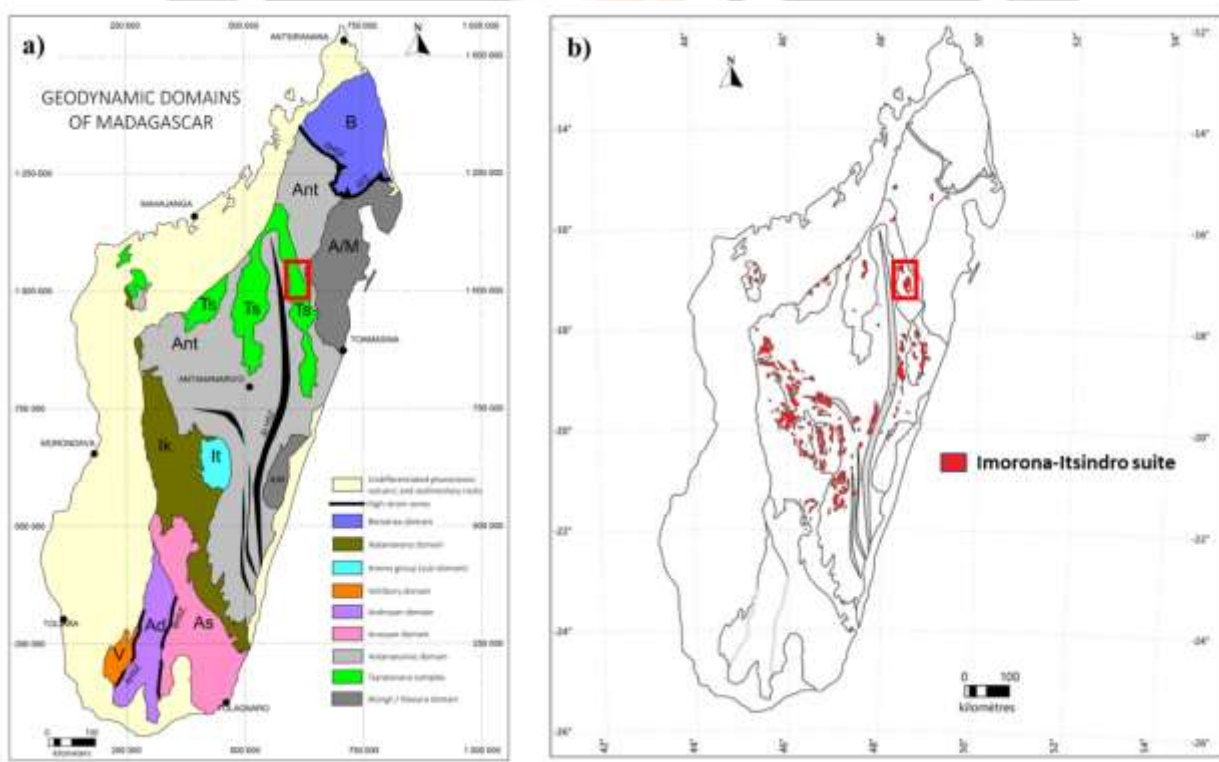


**Fig - 1:** (a) Tectono-metamorphic representation of the Malagasy Precambrian basement, delineating eight geodynamic domains: Antongil-Masora (A/M), Antananarivo (Ant), Itremo (It), Ikalamavony (Ik), Androyan (An), Anosyan (As), Vohibory (V), and Bemarivo (B), and the complex of Tsaratanana (Ts). (b) Schematic representation of the Imorona-Itsindro plutonic suite, with modifications based on Roig et al. (2012) and Tucker et al. (2012) [8]. The red rectangles indicate the location of the study area.

Our study focuses on the tectono-metamorphic domains of Antongil and Antananarivo, the plutonic suites of Imorona-Itsindro and Ambalavao-Kiangara-Maevarano, as well as the volcanic outpourings and quaternary alluvium constituting the Alaotra sedimentary basin (Fig - 2). In this area, the Antongil domain is formed mainly by migmatitic orthogneisses of the Nosy Boraha suite (3.3-3.1 Ga), schists and paragneisses of the Ambodirina group (2.8-2.5 Ga) [8]. The Antananarivo domain is constituted by the tonalitic to dioritic orthogneisses as well as the granitic and granodioritic orthogneisses of the Betsiboka suite (2.8-2.5 Ga), the basic orthogneisses of the Tsaratanana complex (2.8 -2.5 Ga), the paragneisses of Ranomafana east and the Andasibe paragneisses and schists of the Manampotsy group (0.8-0.65 Ga) [8]. Subsequently, the geological formations of the Antongil and Antananarivo domains were intruded by the Imorona-Itsindro plutonic suites (0.8-0.7 Ga) made of the garnet and hornblende orthogneisses of Brickaville and gabbro plutons [8]. The tectonic-magmatic association that generated this suite is controversial. On the one hand, certain studies such as Tucker et al. [3], or Zhou et al. [4], conclude on a context of intraplate magmatism related to a mantle plume. The investigations done by Zhou et al. [4] on gabbros outcropping in the Ambohitsilaozana area, southeast of Alaotra, found trace elements and isotopic compositions consistent with an EM1-type lithospheric mantle source, and an emplacement age between 797 and 772 Ma, respectively. On the other hand, Collins and Windly [5], and Handke et al. (1999) [6] proposed that such chemical fingerprints could be associated to the magmatism of an Andean-type continental arc, when the Mozambican oceanic lithosphere was subducted under the Malagasy continental lithosphere. According to Archibald [1], the plutonic rocks of this reflect bimodal magmatism, with the coexistence of granites, gabbros and syenites, although the latter are less volumetrically representative. According to Roig et al. [8], this suite can be subdivided in four facies: Imorona (II1, comprising granitoids), Itsindro (II2, gabbroic intrusions), Brickaville (II3, including the Brickaville garnet-hornblende orthogneiss), and Ambodilafa (II4, composed of harzburgite, pyroxenite and peridotite). The present research focuses on Itsindro-type gabbros sampled in three distinct sectors, whose description is provided in Section 4. In the Upper Neoproterozoic (0.57-0, 52Ga), the stratoid granites and syenites of the Ambalavao-Kiangara-Maevarano suite intruded the earlier geological formations, an event associated with the collision between East and West Gondwana [3]. An intracontinental rift linked to the separation of Madagascar from Africa, and afterwards India, formed the Plio-Quaternary sedimentary basin of Alaotra and the lake of the same name (Fig - 2). The resulting tectonic extension also originated the basaltic outpourings in this area [7].

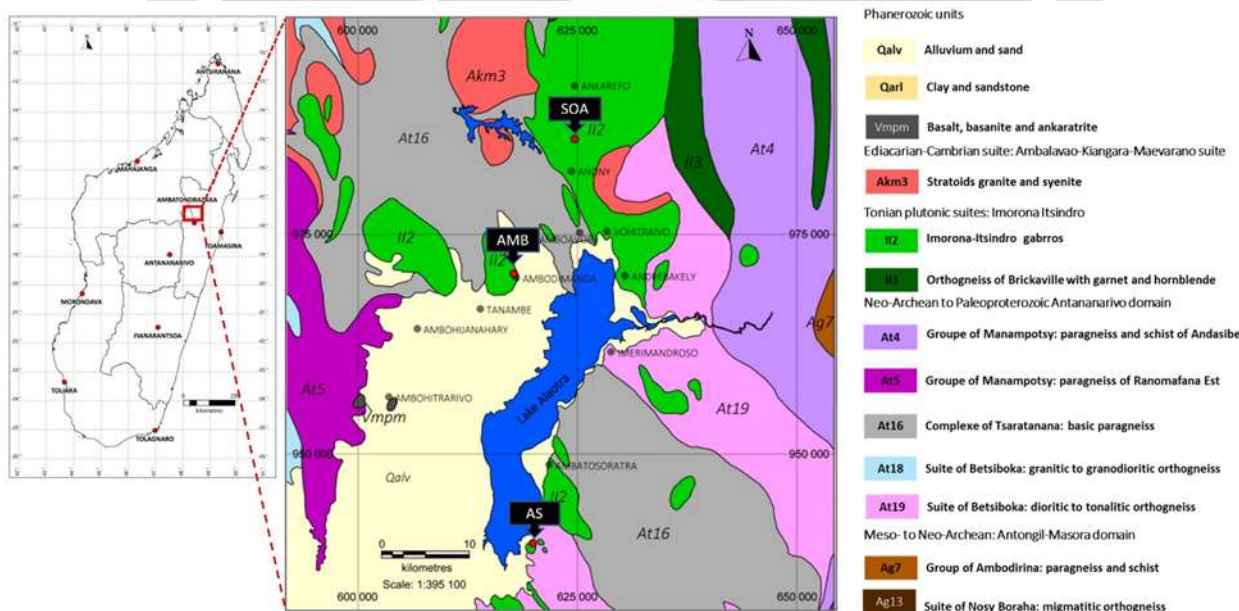


**Fig - 2:** Geological map of the study area modified after Roig et al. [8]. The three sampling locations are represented by red dots. AMB: Ambodimanga, AS Ambatosoratra and SOA: Soavalivato.

### 3. ANALYTICAL METHODS

A total of eight samples, representing the Imorona-Itsindro suite, were selected for both major and trace elements analyses. It includes three from Ambodimanga (GAMB3, M24 and RHT28B), two from Ambatosoratra (AS3 and

AS5) and three from Soavalivato (RHT3A, SOA1 and SOA3). These analyzes were performed by Activation Laboratories Ltd., located in Ontario, Canada. Major elements were measured using an ICP-OES method, involving fusion of 0.2 grams of sample pulp with lithium metaborate/tetraborate. The detection limits range from 0.001 to 0.01%. Additionally, trace element compositions were determined by ICP-MS after the merged samples were diluted in 5% HNO<sub>3</sub>. The sequence of samples that underwent analysis consisted of calibration and verification standards, as well as reagent blanks. Reported detection limits for trace elements ranged from 0.01 to 0.5 parts per million (ppm).

#### 4. RESULTS

Samples were collected from three distinct sectors, as illustrated in Fig - 2. The first sector is located in Ambodimanga at coordinates 17°20'31.22"S and 48°29'23.69"E (Fig - 3c.). The second sector, as shown in Fig - 3a, is situated in Soavalivato at coordinates 17°12'3.40"S and 48°33'8.98"E. The third sector can be found in Ambatosoratra, specifically at coordinates 17°37'21.00"S and 48°30'49.26"E (Fig - 3b).



**Fig - 3:** Gabbro outcrops in the artisanal quarries of Soavalivato (a), Ambatosoratra (b), and Ambodimanga (c).

##### 4.1 Petrographic description

The eight samples present the same petrographic characteristics; indeed, the studied gabbroic rocks are composed essentially of plagioclase, olivine, clinopyroxene and orthopyroxene (Fig - 4a). The accessory minerals include ilmenite, spinel, pyrite, and micron-sized crystals of apatite found in the form of inclusions, particularly within plagioclase (Fig - 4b). Plagioclases are more predominant and coarser than other minerals, varying in size between 5 and 10 mm in diameter. The olivines are less abundant and have a grain size close to 5 mm in diameter. The clinopyroxenes are identified as diopsides, while the orthopyroxenes are recognized as enstatites. These pyroxenes display crystal shapes that range from subhedral to anhedral, and their sizes extend up to 10 millimeters in diameter. Alteration has occurred within these pyroxenes, leading to the formation of secondary amphiboles, notably hornblendes (Fig - 4b). Coronitic textures have additionally been discerned in certain samples, where a core of olivine is surrounded by symplectites composed of the intergrowth of orthopyroxene, clinopyroxene, and spinel. These symplectites are further encompassed by another set composed of the intergrowth of spinels and hornblendes (Fig - 4c). The mineralogical features of these coronas in the gabbros will be the focus of a future study.

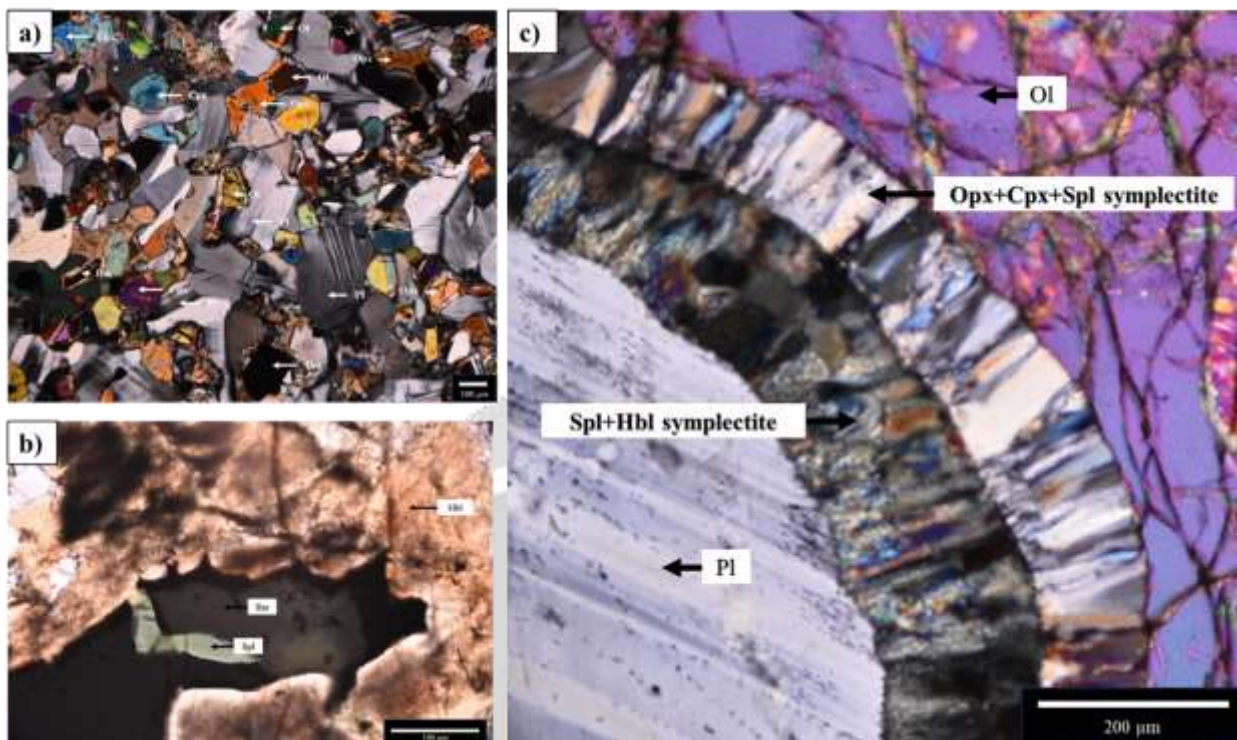


**Fig - 4:** Microscopic insights into Alaotra gabbro thin sections. a) Cross-polarized image providing a detailed view of the gabbro's overall structure and mineral composition from Alaotra. Key components include plagioclase (Pl), olivine (Ol), orthopyroxene (Opx), clinopyroxene (Cpx), and ilmenite (Ilm). b) Plane-polarized image highlighting spinels (Spl) and ilmenite (Ilm) inclusions in the Alaotra gabbro thin section. Additionally, the image showcases the secondary formation of hornblendes resulting from the alteration of pyroxenes. c) Cross-polarized image revealing a distinctive coronitic texture in the gabbro thin section from Alaotra. This texture is characterized by a central olivine (Ol) core enveloped by symplectites comprising orthopyroxene (Opx), clinopyroxene (Cpx), and spinels. Another variant of symplectite comprises spinels and hornblendes. The rock's cumulus component primarily consists of plagioclase (Pl).

#### 4.2. Whole rock geochemistry

The results of the whole rock analyses are reported in table 1 where the elements Be, As, Nb, Mo, Ag, In, Sn, Sb, W, Tl, Pb, and Bi are close to or below the detection limit and were excluded from Table - 1.

**Table - 1:** Whole rock compositions of gabbros from Ambodimanga, Soavalivato and Ambatosoratra.

Localities Samples ID	GAMB3	Ambodimanga M24	RHT28B	RHT3A	Soavalivato SOA1	SOA3	Ambatosoratra AS3	AS5
<b>Major oxides (wt%)</b>								
SiO <sub>2</sub>	48.15	48.46	55.53	46.75	49.51	48.30	48.32	49.46
TiO <sub>2</sub>	0.28	0.21	1.34	0.58	0.42	0.25	0.52	1.25
Al <sub>2</sub> O <sub>3</sub>	16.85	20.68	14.65	15.19	17.58	19.86	20.38	8.77
Fe <sub>2</sub> O <sub>3</sub> <sup>T</sup>	8.60	6.78	11.57	11.61	7.12	7.26	8.44	11.00
MnO	0.12	0.09	0.14	0.17	0.14	0.10	0.12	0.17
MgO	12.04	8.10	5.16	11.85	9.01	10.55	8.66	9.80
CaO	9.95	10.33	5.73	10.83	12.54	10.62	9.65	17.32
Na <sub>2</sub> O	2.49	3.08	3.01	1.87	2.62	2.52	2.96	1.44
K <sub>2</sub> O	0.07	0.10	0.95	0.07	0.08	0.07	0.26	0.25
P <sub>2</sub> O <sub>5</sub>	0.02	0.02	0.18	0.02	0.02	0.01	0.07	0.03
Total	99.23	98.88	98.60	98.63	99.40	99.66	99.62	100.50
LOI	0.67	1.03	0.34	-0.3	0.38	0.11	0.25	0.98
FeOt	7.73	6.10	10.40	10.44	6.40	6.53	7.59	9.89
Fe <sub>2</sub> O <sub>3</sub>	2.30	1.77	3.21	3.22	1.87	1.91	2.25	3.03

FeO	5.83	4.63	7.74	7.76	4.86	4.95	5.73	7.38
Mg#	73.52	70.32	46.93	66.93	71.50	74.24	67.05	63.85
<b>Trace elements (ppm)</b>								
Sc	21	13	28	32	35	15	11	57
V	100	61	259	175	169	70	79	348
Cr	150	120	160	690	360	170	80	70
Co	58	45	39	59	38	48	49	43
Ni	230	220	100	310	180	270	310	250
Cu	110	70	80	40	60	80	50	40
Zn	50	40	120	70	50	60	60	70
Ga	12	14	19	13	14	12	13	15
Ge	1	0.9	1.5	1.2	1.2	0.9	0.9	2
Rb	1	1	20	1	1	-	3	5
Sr	264	348	401	158	265	288	378	122
Y	5.6	4.1	20.2	12.6	11.1	4.9	6.8	20.9
Zr	11	8	107	21	14	10	35	70
Cs	0.1	0.1	-	0.1	0.1	-	0.1	0.3
Ba	12	20	964	21	31	32	118	118
La	0.59	1.06	27.2	0.84	0.78	1.03	3.42	5.15
Ce	1.66	1.74	50	2.47	2.3	2.4	7.14	12.6
Pr	0.27	0.35	5.74	0.47	0.43	0.32	0.94	1.96
Nd	1.88	1.8	23.7	2.76	2.54	1.85	4.4	10
Sm	0.58	0.56	5.15	1.14	1.08	0.58	1.11	3.31
Eu	0.46	0.485	1.31	0.58	0.664	0.486	0.573	1.1
Gd	0.83	0.71	4.67	1.82	1.54	0.7	1.23	3.88
Tb	0.17	0.12	0.69	0.34	0.28	0.13	0.2	0.63
Dy	1.09	0.77	3.96	2.22	2.03	0.86	1.23	4.07
Ho	0.22	0.16	0.75	0.48	0.42	0.19	0.25	0.82
Er	0.63	0.47	2.13	1.39	1.19	0.54	0.76	2.31
Tm	0.09	0.068	0.302	0.201	0.167	0.076	0.109	0.351
Yb	0.57	0.42	1.9	1.27	1	0.5	0.69	2.18
Lu	0.08	0.06	0.29	0.19	0.15	0.08	0.11	0.35
Hf	0.40	0.30	3.00	0.80	0.60	0.30	0.80	2.70
Ta	0.03	0.03	0.19	0.02	1.33	0.03	0.42	0.11
U	0.01	0.01	0.05	-	0.01	0.06	0.06	0.12
$\Sigma$ REE	9.12	8.77	127.79	16.17	14.57	9.74	22.16	48.71
$(\text{Eu}/\text{Eu}^*)_{\text{N}}$	2.02	2.35	0.82	1.23	1.57	2.33	1.50	0.94
$(\text{La}/\text{Yb})_{\text{N}}$	0.70	1.72	9.74	0.45	0.53	1.40	3.37	1.61
$(\text{La}/\text{Sm})_{\text{N}}$	0.63	1.16	3.25	0.52	1.37	0.45	1.90	0.96

#### 4.2.1. Major elements

The studied samples show a homogeneous composition in  $\text{SiO}_2$  which varies from 46.75 to 55.53%, and Mg# is relatively high ( $46.93 < \text{Mg}\# < 74.24$ ). According to the classification scheme of Le Maître [9] shown in Chart - 1, most of the samples reveal low alkalis content ( $\text{Na}_2\text{O} + \text{K}_2\text{O}$ : 1.14 - 3.22%) and are therefore classified as sub-alkaline gabbros. However, RHT28B is in the gabbroic-diorite domain. The examination of Harker diagrams comparing #Mg concentration with other major oxides indicates the emergence of distinct trends (Chart - 1). Primarily, the gradual depletion in Mg# compared to  $\text{SiO}_2$  is a telltale sign of olivine and clinopyroxene fractionation, underscoring the selective removal of magnesium-rich phases (Chart - 2a). Secondly, the gradual increment of Mg# alongside CaO points to the fractionation of clinopyroxene and plagioclase (Chart - 2c). This suggests that these minerals are preferentially crystallizing from magma. Similarly, the gradual increment of Mg# alongside  $\text{Al}_2\text{O}_3$  also reflects the fractionation of clinopyroxene and plagioclase, as well as spinel, reinforcing the notion that these minerals play a significant role in the chemical evolution of the rock (Chart - 2b). On the other hand, the depletion of  $\text{TiO}_2$  in relation to the Mg# concentration reveals an interesting aspect of the composition of the rock (Chart - 2f). This indicates that titanium-rich oxides, such as ilmenite, are present because they consume titanium during their formation. The reduction in  $\text{TiO}_2$  content relative to #Mg serves as evidence for the incorporation of these oxides into the crystalline phases of the rock, further elucidating the complex mineralogical transformations occurring during rock crystallization. Conversely, the enrichment in  $\text{Na}_2\text{O}$  and  $\text{K}_2\text{O}$  within Harker diagrams indicates residual enrichment in the melt, highlighting that these elements remain in the liquid phase, reflecting their limited involvement in the crystallization process (Chart - 2d, e).

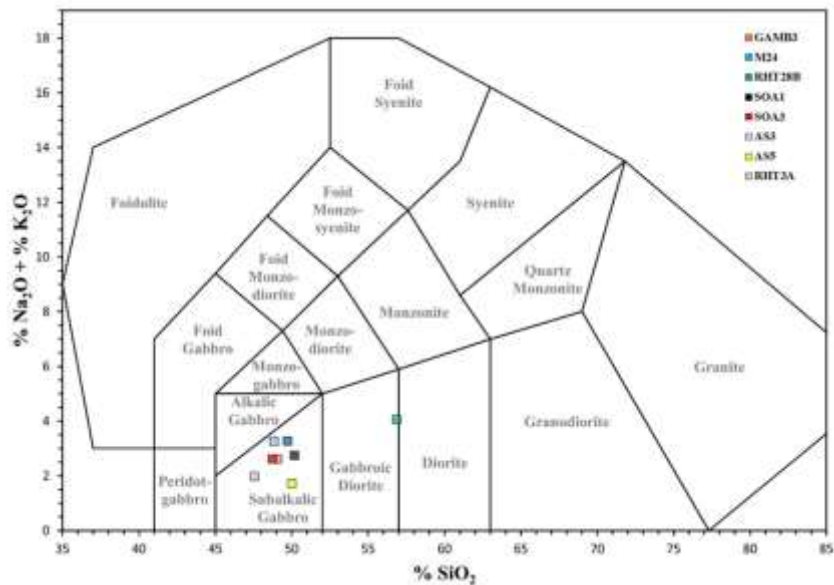


**Chart - 1:** Total alkalis (Na<sub>2</sub>O + K<sub>2</sub>O) vs. SiO<sub>2</sub> Classification diagrams of gabbros from Ambodimanga, Ambatosoratra and Soavalivato according to the scheme of Le Maître [9].

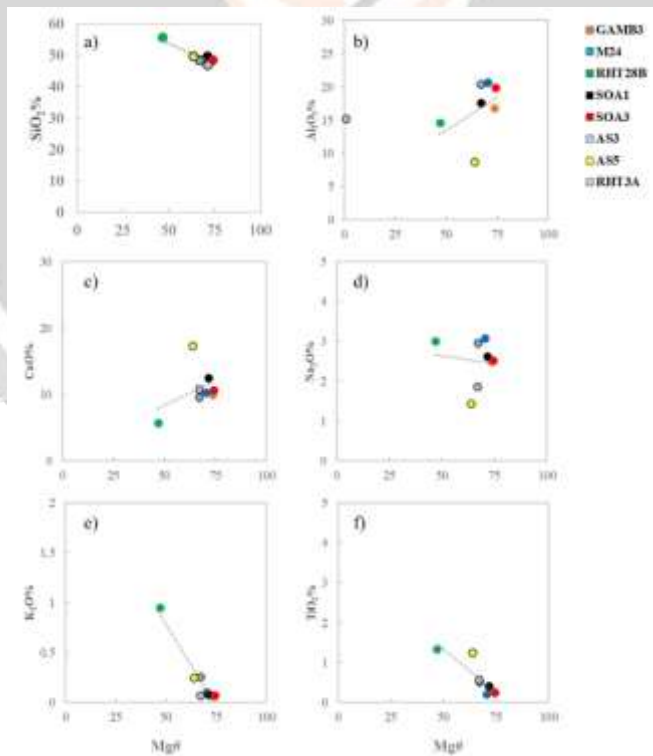


**Chart - 2:** Harker diagrams illustrating variations in Mg# relative to major oxide compositions in Alaotra gabbros.

#### 4.2.2. Trace elements

**Rare Earth Elements (REE):** the REE patterns diagram (Chart - 3) is normalized to the N-MORB according to Sun and McDonough [10]. GAMB3, M24, SOA1, SOA3, and RHT3A REEs are characterized by a relatively flat pattern that reflects a common origin. The REE profile of AS5 is also flat but shows a very slight Light Rare Earth Elements (LREE) enrichment, while the profiles of the RHT28B and AS3 samples show a strong LREE enrichment. The ratio  $(\text{La}/\text{Sm})_{\text{N}}$  ratio (Table - 1) ranges between (0.45-1.90). This ratio is greater than one in samples M24, RHT28B, SOA3 and AS3, reflecting the enrichment of the LREE content. However, it is less than one in RHT3A, SOA1 and AS5, indicating LREE depletion. The  $(\text{La}/\text{Yb})_{\text{N}}$  ratio for most samples (except RHT28B), varies between (0.45-3.37) indicating the depletion of these rocks in LREE compared to HREE, while RHT28B having a relatively high ratio reflects the enrichment of LREE relative to HREE. RHT28B and AS5 have slight negative anomalies in  $(\text{Eu}/\text{Eu}^*)_{\text{N}}$ , respectively 0.82 and 0.94 indicating plagioclase accumulation due to magmatic processes. Although most samples show positive anomalies, reflecting plagioclase fractionation.

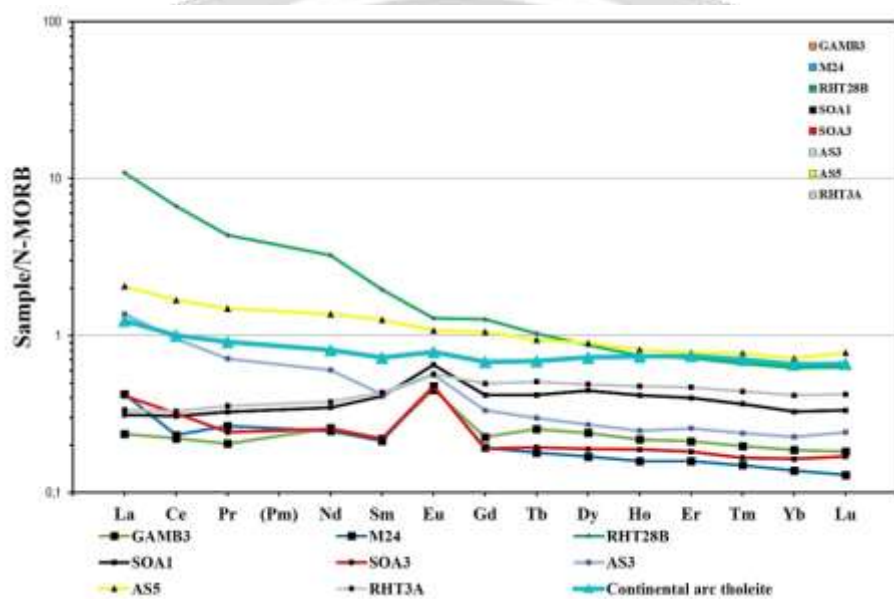


**Chart - 3:** Rare Earth Element (REE) patterns of the Alaotra gabbros normalized against N-MORB values according to Sun and McDonough [10].

**Large Ion Lithophile Elements (LILE):** the Strontium (Sr) variation plots against #Mg shows a clear negative correlation (Chart - 4a) indicating that strontium (Sr) is associated with felsic minerals which are plagioclase [11]. Rubidium (Rb) and Barium (Ba) compared to #Mg show continuous trends (Chart - 4b, c). However, in comparison to other samples, Rb and Ba concentrations in RHT28B are higher signifying a more important association with plagioclase. The same statement applies to the case of Cesium (Cs) in the sample AS5 (Chart - 4d).

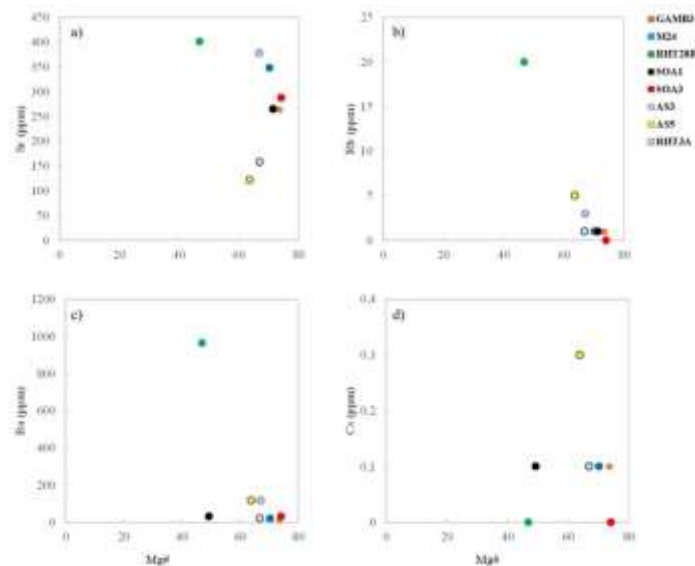


**Chart - 4:** Variation diagrams depicting Mg# against LILE (Large Ion Lithophile Elements) for the Alaotra gabbros.

**High Field Strength elements (HFSE):** overall the HFSEs show negative trends against #Mg (Chart - 5a, b, c), this implies their occurrence in Fe-rich minerals. A good positive correlation is also shown by zirconium (Zr), hafnium (Hf), Ytterbium (Y) (Chart - 6) which deduces their mutual existence from the fractional crystallization of a common mafic magma [12].

The multi-element diagram (Chart - 7) is normalized to the N-MORB according to Sun and McDonough [10] GAMB3, M24, SOA1, SOA3 and RHT3A shows profiles typical of continental arc tholeiite, with remarkable positive Cs, Sr, K, Sr, Ba anomalies and notable negative uranium (U), tantalum (Ta), and phosphorus (P) anomalies. AS5 profile is also flat but shows an anomaly in Ba as well as strong depletions in P and niobium (Nb). The RHT28B and AS3 samples profiles show high enrichment in LILEs (especially in Ba) relative to the HFSEs (Chart - 7).

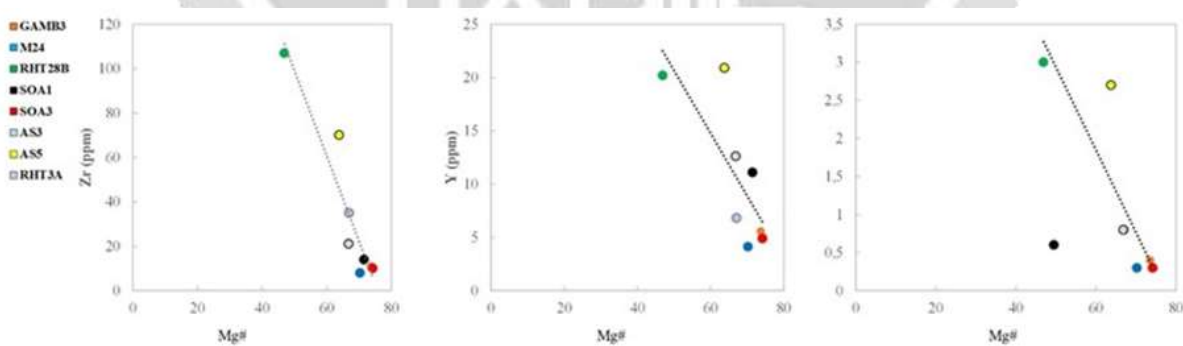


**Chart - 5:** Variation diagrams illustrating Mg# to HFSE (High Field Strength Elements) in the Alaotra gabbros.

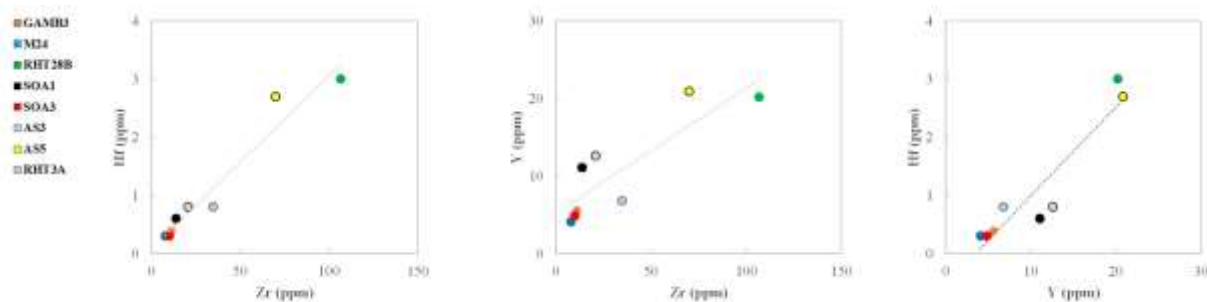


**Chart - 6:** Zr vs. Hf, Zr vs. Y, and Y vs. Hf variation diagrams of Alaotra gabbros.

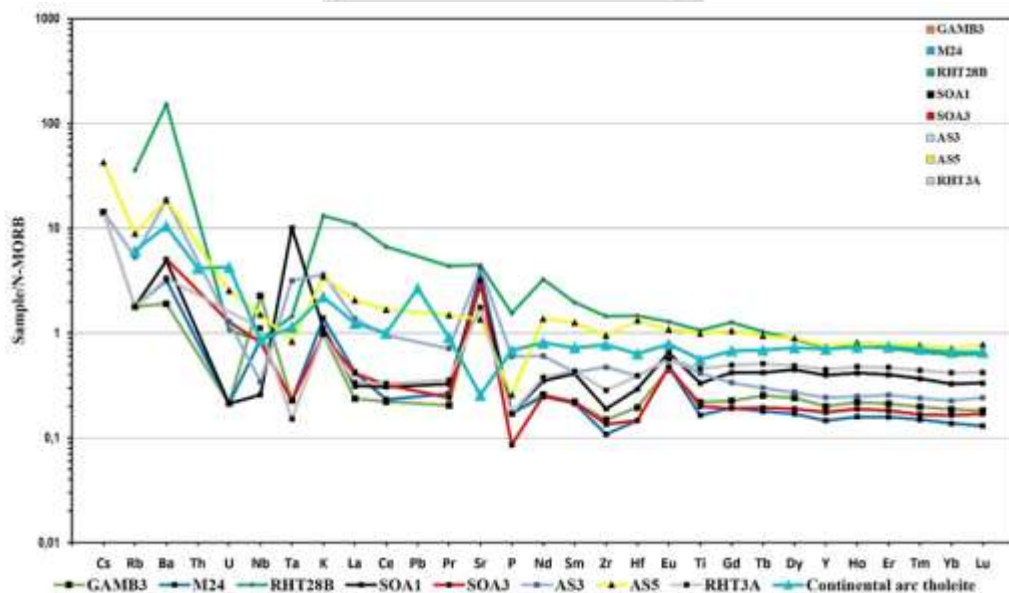


**Chart - 7:** Multi-element diagram of the Alaotra gabbros normalized against N-MORB values according to Sun and McDonough [10].

#### 4.2.3. Tectonic discriminants

By applying the ternary diagram ( $Ti/100$  vs.  $Zr$  vs.  $Y^{x^3}$ ) discriminating mafic rocks from Pearce and Cann [13], the samples are found in three distinct settings: island arc (GAMB3, M24, SOA1, SOA3, and RHT3A), ocean floor basalts + island arc + calc-alkaline (AS5), and within plate for samples RHT28B and AS3 (Chart - 8a). Additionally, the binary diagram ( $Ti/Y$  vs.  $Zr/Y$ ) of Pearce and Gale [14] shows that most samples are from an active plate margin, except RHT28B and AS3 which are from an intraplate magmatism (Chart - 8c). Moreover, the discriminating ternary diagram ( $TiO_2$  vs.  $MnO^{x10}$  vs.  $P_2O_5^{x10}$ ) of Mullen [15] suggests that the rocks of GAMB3, M24, SOA1, SOA3, and RHT3A were formed in a context of boninite (Chart - 8b), while the others were formed rather either in the island arc (case of AS3 and AS5), or Mid Oceanic Ridge Basalt (MORB, case of RHT28B).

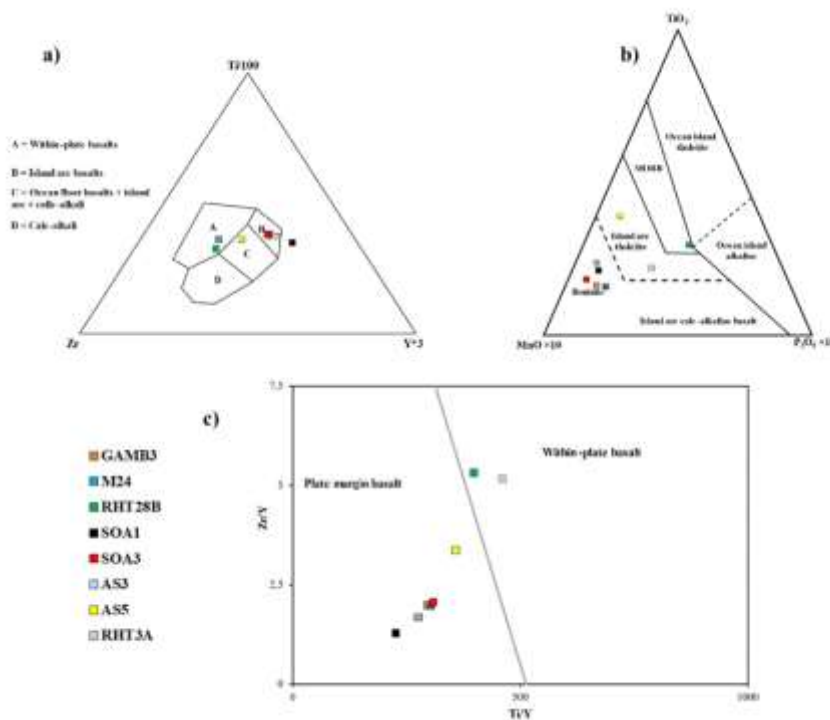


**Chart - 8:** Tectonic discriminant diagrams for the Alaotra gabbros. (a)  $\text{Ti}/100$  / ( $\text{Zr}$  vs.  $\text{Y}^{x3}$ ) ternary diagram based Pearce & Cann [13]; b)  $\text{TiO}_2$  / ( $\text{Mn} \times 10$  vs.  $\text{P}_2\text{O}_5 \times 10$ ) ternary diagram following Mullen [15]; c)  $\text{Ti}/\text{Y}$  vs.  $\text{Zr}/\text{Y}$  binary diagram according to Pearce & Gale [14].

## 5. DISCUSSIONS

### 5.1. Discriminant series and magmatic affinity

Firstly, the results emphasize the "Tholeiitic Affinity" of the gabbro samples, established through their relatively high  $\text{MgO}$  content and intermediate values in  $\text{FeOt}$  (6.1-10.44%). This characteristic is effectively depicted using the AFM diagram, introduced by Irvine and Baragar [16] (Chart - 9a). The tholeiitic affinity, a hallmark of rocks formed in oceanic settings, is indicative of specific chemical compositions that define the gabbro samples. Besides, the confirmation of this affinity is underscored as another binary diagram created by Winchester and Floyd [17] lends further support to this classification (Chart - 9b). The diagram accounts for low  $\text{TiO}_2$  contents (0.208-1.342%) and distinct  $\text{Zr}/\text{P}_2\text{O}_5$  ratios (0.04-0.23), which align with the tholeiitic nature of the gabbro samples.

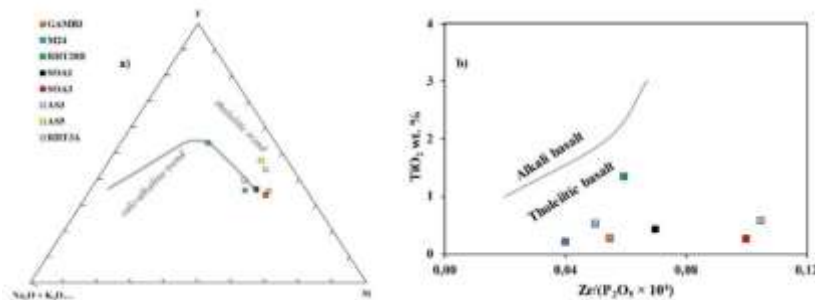


**Chart - 9:** Discriminant diagrams of gabbros from Alaotra. (a) AFM ( $\text{FeOt}$  vs.  $\text{MgO}$  vs.  $\text{SiO}_2$ ) based on Irvine and Baragar [16], (b)  $\text{Zr}/(\text{P}_2\text{O}_5 \times 10^4)$  vs.  $\text{TiO}_2$  according to Winchester and Floyd [17].

Secondly, the Pearson-type spider diagram, as represented in Chart - 10, contributes additional insights. It shows uneven distributions of elements, underlining varied profiles. Furthermore, it unveils a noticeable decoupling effect, emphasizing the enrichment in more mobile Large Ion Lithophile Elements (LILE). This enrichment is discerned through pronounced positive anomalies in elements such as Sr, K, Rb, and Ba. These patterns offer crucial evidence pointing to the involvement of a fluid phase, a feature linked to fluid-assisted fusion related to subduction processes. The notable depletion in phosphorus (P) observed in the samples is explained as the result of the fractionation of apatite.

Moreover, in the case of samples RHT28B and AS3, there appears to be an enriched source of Light Rare Earth Elements (LREE) that is relatively incompatible (Chart - 10). This source could be linked to either an enriched mantle of deep origin or a combination of an E-MORB-like source influenced by MASH processes along with some degree of crustal contamination. The multi-element diagram also reveals these evident indications of crustal contamination. Additionally, the increase in alkaline elements, resulting from either the fractionation of the initial melt during the process of fractional crystallization or through crustal contamination following the assimilation of felsic enclaves during the intrusion, could plausibly elucidate the abundance of feldspar, particularly in these two samples.

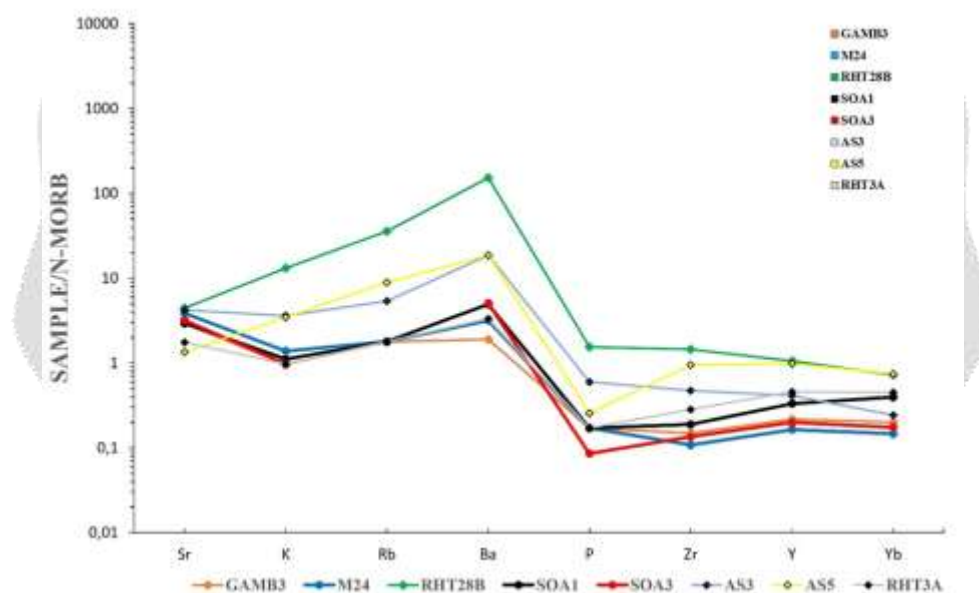


**Chart - 10:** Pearson-type spider diagram comparing the LILEs and HSFEs of the Alaotra gabbros. The diagram is N-MORB normalized as per Sun and McDonough [10] and the number of elements used was limited by the data availability.

Finally, heavy rare earth elements (HREE) do not show signs indicative of a deep mantle source, such as negative slopes associated with the source where the garnet was fractionated (Chart - 3), further supporting the potential gabbroic under-plate remelting scenario (Fig - 5b). Hence, these gabbros originate from both enriched and depleted tholeiitic sources, and the variations in composition among samples within the same intrusion could likely be attributed to the effects of fractional crystallization.

In sum, the analysis of the gabbro samples encompasses their tholeiitic affinity, the involvement of fluid phases linked to subduction zone, the gabbroic under-plate melting source, the role of crustal contamination, fractional crystallization, and the enrichment of alkaline elements.

## 5.2. Tectonic and geodynamic setting

Given the common origin of gabbro samples from a tholeiitic source and the variations observed in tectonic discriminants and trace element signatures, it is reasonable to infer that their geological setting corresponds to a subduction zone. In this subduction zone environment, a complex process can be imagined. It involves the subduction of Mozambican oceanic lithosphere, which moves eastward beneath the Malagasy Precambrian basement (Fig - 5a, b). The latter includes the tectono-metamorphic domains of Anosyan, Ikalamavony, Antananarivo and Antongil-Masora and existed between 0.84 and 0.76 billion years ago. In this subduction zone, the Mozambican oceanic plate interacts with the overlying mantle, contributing to the release of water that triggers mantle melting. This process leads to the formation of a large volume of basaltic melt within the asthenosphere (Fig - 5b). According to a widely accepted petrogenetic model, this fluid-assisted melting of the mantle generates basaltic magmas, which rise and amalgamate at the base of the continental crust. Here they undergo fractional crystallization, resulting in the formation of gabbros by progressive solidification and gravitational sedimentation of olivines, pyroxenes and plagioclases in a magma chamber. These gabbros exhibit distinctive features, including cumulative textures and decoupling of large fluid ion lithophile elements (LILE) and high field intensity elements (HFSE), which are typical features of subduction zones. Additionally, the high rare earth element (HREE) content suggests a low subduction angle (absence of garnet in the source), implying an Andean-type subduction zone scenario.

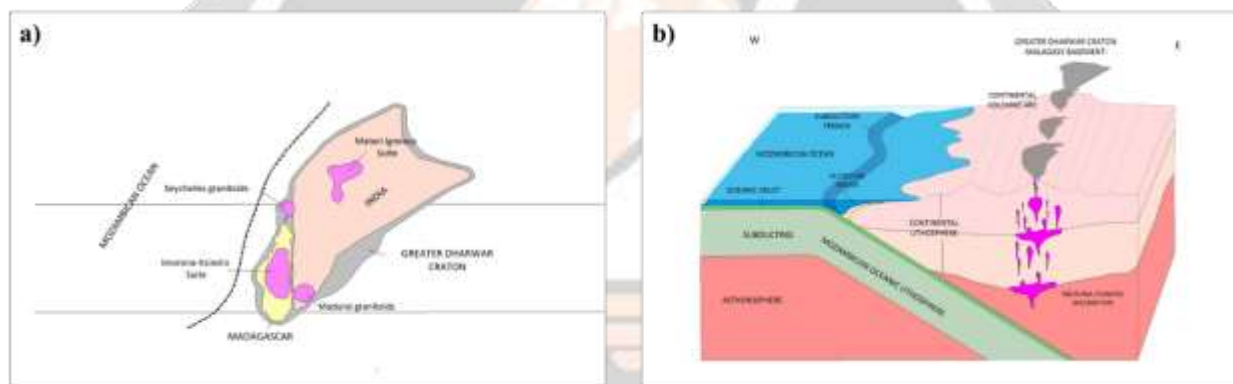


**Fig - 5:** (a) Paleogeographic map illustrating the Andean-type magmatic arc, depicting the eastward subduction of Mozambican oceanic lithosphere beneath the Malagasy basement. The latter is identified as part of the Greater Dharwar craton during the Rodinia rifting, with modifications based on Piper [18] and Zhou [4]. (b) Proposed 3-D model representing the Imorona-Itsindro magmatism associated with subduction processes.

## 5. CONCLUSIONS

The whole rock analyses of Cryogenian gabbros from the Imorona-Itsindro plutonic suite in the Alaotra region of Madagascar has provided essential information on their geological origins. First, these gabbros initially exhibit tholeiitic characteristics, but subsequent geological processes, including fractional crystallization and contamination, caused them to evolve into a calc-alkaline composition. Additionally, geochemical data indicate a tectonic environment associated with subduction. This evidence strongly supports the idea that these gabbros originate from an underplate magma source located in the upper mantle. This source is the result of eastward subduction of Mozambican oceanic lithosphere beneath Malagasy continental lithosphere approximately 0.8 to 0.7 billion years ago. Most notably, the results of this study provide substantial support for the Andean-type continental arc model, rather than the mantle plume theory as the most likely geological explanation for the formation of these gabbros.

## 5. ACKNOWLEDGEMENT

Geochemical data were plotted using the excel spread sheets of Marshall and Daniel (1996).

## 6. REFERENCES

- [1] D. B. Archibald *et al.*, “Genesis of the Tonian Imorona–Itsindro magmatic Suite in central Madagascar: Insights from U–Pb, oxygen and hafnium isotopes in zircon,” *Precambrian Res.*, vol. 281, pp. 312–337, Aug. 2016, doi: 10.1016/j.precamres.2016.05.014.
- [2] R. D. Tucker *et al.*, “Neoproterozoic extension in the Greater Dharwar Craton: a reevaluation of the ‘Betsimisaraka suture’ in Madagascar This article is one of a series of papers published in this Special Issue on the theme of *Geochronology* in honour of Tom Krogh.,” *Can. J. Earth Sci.*, vol. 48, no. 2, pp. 389–417, Feb. 2011, doi: 10.1139/E10-034.
- [3] R. D. Tucker, J. Y. Roig, B. Moine, C. Delor, and S. G. Peters, “A geological synthesis of the Precambrian shield in Madagascar,” *J. Afr. Earth Sci.*, vol. 94, pp. 9–30, Jun. 2014, doi: 10.1016/j.jafrearsci.2014.02.001.
- [4] J.-L. Zhou, S. Shao, Z.-H. Luo, J.-B. Shao, D.-T. Wu, and V. Rasoamalala, “Geochronology and geochemistry of Cryogenian gabbros from the Ambatondrazaka area, east-central Madagascar: Implications for Madagascar-India correlation and Rodinia paleogeography,” *Precambrian Res.*, vol. 256, pp. 256–270, Jan. 2015, doi: 10.1016/j.precamres.2014.11.005.
- [5] A. S. Collins and B. F. Windley, “The Tectonic Evolution of Central and Northern Madagascar and Its Place in the Final Assembly of Gondwana,” *J. Geol.*, vol. 110, no. 3, pp. 325–339, May 2002, doi: 10.1086/339535.
- [6] M. J. Handke, R. D. Tucker, and L. D. Ashwal, “Neoproterozoic continental arc magmatism in west-central Madagascar.,” *Geology*, vol. 27, pp. 351-354., 1999.
- [7] T. M. Kusky, E. Toraman, T. Raharimahefa, and C. Rasoazanamparany, “Active tectonics of the Alaotra–Ankay Graben System, Madagascar: Possible extension of Somalian–African diffusive plate boundary?,” *Gondwana Res.*, vol. 18, no. 2–3, pp. 274–294, Sep. 2010, doi: 10.1016/j.gr.2010.02.003.
- [8] J.-Y. Roig, R. D. Tucker, S. G. Peters, C. Delor, and H. Théveniaut, “Carte géologique de la République de Madagascar,” Madagascar, 2012.
- [9] R. W. Le Maitre, *Igneous rocks: a classification and glossary of terms : recommendations of the International Union of Geological Sciences, Subcommission on the Systematics of Igneous Rocks*, 2nd ed. Cambridge, U.K.: Cambridge University Press, 2002.
- [10] S. Sun and W. F. McDonough, “Chemical and isotopic systematics of oceanic basalts: implications for mantle composition and processes. In: A.D. Saunders & M.J. Norry (Editors), *Magmatism in the Ocean Basins*,” *Geol. Soc. Lond. Spec. Publ.*, vol. 42, pp. 313–345, 1989.
- [11] B. Mason and C. B. Moore, *Principles of Geochemistry*., John Wiley and Sons, 1982.
- [12] M. Wilson, *Igneous Petrogenesis, A Global Tectonic Approach*. Unwin Hyman, London, 1989.
- [13] J. A. Pearce and R. J. Cann, “Tectonic setting of basic volcanic rocks determined using trace element analyses,” *Earth Planet. Sci. Lett.*, vol. 19.2, pp. 290–300, 1973.
- [14] J. A. Pearce and G. H. Gale, “Identification of ore-deposition environment from trace-element geochemistry of associated igneous host rocks,” *Geol. Soc. Lond. Spec. Publ.*, vol. 7.1, pp. 14–24, 1977.
- [15] E. D. Mullen, “Earth and Planetary Science Letters,” *Earth Planet. Sci. Lett.*, vol. 62.1, pp. 53–62, 1983.
- [16] T. N. Irvine and W. R. A. Baragar, “A guide to the chemical classification of the common volcanic rocks,” *Can J Earth Sci*, vol. 8, pp. 523-548., 1971.
- [17] J. A. Winchester and P. A. Floyd, “Geochemical magma type discrimination: application to altered and metamorphosed basic igneous rocks,” *Earth Planet. Sci. Lett.*, vol. 28.3, pp. 459–469, 1976.
- [18] J. D. A. Piper, “Discussion on ‘The making and unmaking of a supercontinent: Rodinia revisited’ by J.G. Meert and T.H. Torsvik, *Tectonophysics*, 375 (2003) 261–288,” *Tectonophysics*, vol. 383, no. 1–2, pp. 91–97, May 2004, doi: 10.1016/j.tecto.2004.03.004.